INTERFERENCE-AWARE RECEIVER DESIGN FOR MU-MIMO IN LTE: REAL-TIME PERFORMANCE MEASUREMENTS

Contributors

Sebastian Wagner
Intel Mobile Communications

Florian Kaltenberger
EURECOM

Multiuser (MU) MIMO is a promising technique to significantly increase the cell capacity in LTE systems. However, users scheduled for MU-MIMO may still experience strong MU interference if the channel state information at the base station is outdated or in small cells with a limited number of users available. To tackle the MU interference, an interference-aware (IA) receiver design is employed. Unlike the interference-unaware (IU) receiver, the IA receiver exploits the information about the interfering data stream in the decoding process, resulting in a significant performance gain while maintaining a moderate complexity. We evaluate the performance of both receivers in terms of throughput through real-time measurements carried out with the OpenAirInterface, an open-source hardware/software development platform created by EURECOM. The measurement results show that the IA receiver achieves significantly higher data rates compared to the IU receiver if the user has multiple receive antennas.

Introduction

It is well known that multiuser (MU) multiple-input multiple-output (MIMO) transmission can significantly increase the cell throughput compared to single-user (SU) MIMO transmission due to MU diversity. Therefore, MU-MIMO is already implemented in the 3GPP long-term evolution (LTE) standard Release 8[1], where it is referred to as transmission mode (TM) 5. However, since TM5 only supports two co-scheduled user equipment (UEs) with a single data stream each, the MU-MIMO mode has been extended in TM8 and TM9 in LTE Release 9 and 10, respectively, by introducing UE-specific (precoded) reference signals (RS).[2][3] In TM8 and TM9 the base station (referred to as eNodeB [eNB] in context of LTE) can schedule up to four users with a single data stream where both precoding technique and number of co-scheduled users are entirely transparent to the UE.

"…MU-MIMO can significantly increase cell throughput compared to SU-MIMO…"

In MU-MIMO, the throughput at the UEs greatly depends on the amount of interference from co-scheduled users. This MU interference can be managed at the eNB through efficient precoding or at the UE via interference cancellation. If the precoding is effective, there will not be any significant MU interference at the UEs and thus no need to cancel that residual interference. However, in TM5 where the precoding is based on a very limited set of possible precoding vectors, efficient precoding can only be achieved if the number of users in the cell is large. The same holds true for non-codebook–based precoding schemes as enabled in TM8 and TM9, unless very accurate channel state information is available at the eNB, which in turn is very difficult to obtain.

"…The throughput at the UEs greatly depends on the amount of interference from co-scheduled users"

Consequently, the precoding is likely to be incapable of efficiently mitigating the MU interference at the UEs especially in small cells with a very limited number of users. Therefore, it is of paramount importance that the UEs are able to effectively mitigate the residual MU interference by exploiting its structure.

To achieve effective interference mitigation at the UE, different receiver designs have been proposed in the literature. Ghaffar and Knopp[4] propose an optimal simplified interference-aware (IA) receiver based on the maximum likelihood (ML) criterion. However, the optimal IA receiver requires knowledge of the interfering symbol constellation, which is unavailable to the UE. Therefore, Ghaffar and Knopp[4] propose to use a fixed constellation and show that the performance degradation of the sub-optimal IA receiver is acceptable. Bae et al.[5] try to overcome this disadvantage of the IA receiver by implementing an interference modulation estimator prior to the IA receiver. It is shown through simulations that this joint receiver outperforms the IA receiver with fixed interfering constellation especially when the interference power is high. The question of the performance-complexity tradeoff of different receivers is addressed by Bai et al.[6], where a linear receiver termed interference rejection combiner (IRC) is applied to MU-MIMO. Based on simulation results under various channel conditions, the authors conclude that the IRC achieves the best performance-complexity tradeoff. However, it is important to note that the simulation results of Bai et al.[6] assume an infinite number of potential users with the 4 transmit-antenna codebook suggesting that the MU interference is rather low. Under higher interference levels, the simulation results of Bae et al.[5] show a significant performance loss of the IRC compared to the IA receiver. However, in practice, the amount of MU interference is highly dependent on the algorithms (scheduling, precoding, and so on) implemented at the eNB and it is therefore difficult to identify a "typical" MU-MIMO scenario.

In this article, we focus on TM5 applied to small-cell scenarios with *few* users in the cell and the two transmit-antenna codebook resulting in *high* residual MU interference at the UEs. The focus on TM5 is further motivated by the fact that at lower bandwidths (5 MHz and lower), the number of possible UE-specific downlink control information (DCI) in the physical downlink control channel (PDCCH) is limited and it is very likely that the eNB is unable to co-schedule more than two UEs. We implemented the IA receiver proposed by Ghaffar and Knopp[4] on the OpenAirInterface real-time platform[7] and evaluate its performance through measurements under realistic channel conditions.

The remainder of the article is organized as follows. The next section, "System Model," introduces the system model and briefly reviews the IA receiver design. In the section "Simulation Results," we carry out simulations to evaluate the IA receiver performance under false assumptions on the interfering symbol constellation. The section "Real-Time Measurements" describes the real-time

"…It is of paramount importance that the UEs are able to effectively mitigate the residual MU interference…"

"We implemented the IA receiver proposed by Ghaffar and Knopp on the OpenAirInterface real-time platform…"

measurement setup and presents our results. Finally, we summarize our results in the "Conclusion" section.

Notation: In the following, boldface lowercase and uppercase characters denote vectors and matrices, respectively. The operators $(\cdot)^H$ and $\|\cdot\|$ denote conjugate transpose and norm, respectively. The $N \times N$ identity matrix is denoted $\mathbf{I}_N$, z^R and z^I are the real and imaginary part of $z \in \mathbb{C}$, respectively. The imaginary unit is denoted $\mathbf{i}$. A random vector $\mathbf{x} \sim \mathbb{NC}\ (\mathbf{m}, \boldsymbol{\Theta})$ is complex Gaussian distributed with mean vector $\mathbf{m}$ and covariance matrix $\boldsymbol{\Theta}$.

System Model

Consider a system with an n_t- antenna eNB and K scheduled UEs, each endowed with n_r receive antennas. We assume that the eNB transmits a *single* data stream s_k to UE $k, (k = 1, 2, \ldots, K)$ and applies a linear precoding technique. Under narrow-band transmission, the received signal $\boldsymbol{y}_k \in \mathbb{C}^{n_r}$ of user k takes the form

$$\boldsymbol{y}_k = \underbrace{\mathrm{H}_k \mathbf{g}_k \mathrm{s}_k}_{\text{useful signal}} + \mathrm{H}_k \underbrace{\sum_{j=1, j \neq k,}^{K} \mathbf{g}_j \mathrm{s}_j}_{\text{MU interference}} + \underbrace{\mathbf{n}_k}_{\text{noise}}$$

where $\mathbf{H}_k = [\mathbf{h}_{k1}, \mathbf{h}_{k2}, \ldots, \mathbf{h}_{kn_r}]^H \in \mathbb{C}^{n_r \times n_t}$ is the channel from the eNB to UE k, $\mathbf{G}_k = [\mathbf{g}_1, \mathbf{g}_2, \ldots, \mathbf{g}_K]^{n_t \times K}$ is the concatenated precoding matrix and $\mathbf{n}_k \sim \mathbb{NC}$ $(0, \sigma^2\ \mathbf{I}_{n_r})$ is the noise vector. Defining the *effective* channels of user k as $\overline{\mathbf{h}}_i \triangleq \mathbf{H}_k \mathbf{g}_i, (i, = 1, 2, \ldots, K)$, the received signal reads

$$\boldsymbol{y}_k = \overline{\mathbf{h}}_k \mathrm{s}_k + \sum_{j=1, j \neq k,}^{K} \overline{\mathbf{h}}_j \mathrm{s}_j + \mathbf{n}_k.$$

> *"The key challenge in MU-MIMO is to minimize the MU interference"*

The key challenge in MU-MIMO is to minimize the MU interference. This interference can be mitigated at the eNB by computing an appropriate precoder $\mathbf{G}$ or the interference can be accounted for in the receiver by exploiting its potential structure. It is well known that efficient interference mitigation at the eNB requires precise downlink channel knowledge, which can only be acquired through extensive user feedback. On the other hand, interference management at the receiver necessitates an estimate of the effective channels $\overline{\mathbf{h}}_i$ as well as the interfering symbol alphabet A_j, $s_j \in A_j (j \neq k)$. The LTE standard defines three possible symbol alphabets $A_k \in \{Q_4, Q_{16}, Q_{64}\}$, that is, QPSK, 16QAM, and 64QAM. In the following sections, we discuss the LTE MU-MIMO mode in more detail.

MU-MIMO in LTE Release 8

LTE Release 8[1] defines MU-MIMO in TM5 where two UEs can be scheduled simultaneously each receiving a *single* data stream. The UEs are aware of a

co-scheduled user through the downlink power offset value signaled in the DCI. Moreover, LTE Release 8 adopts a codebook-based precoding scheme as a compromise between performance and feedback overhead. The codebook Γ for $\boldsymbol{n_t} = \boldsymbol{2}$ is defined as

$$\Gamma = \tfrac{1}{\sqrt{2}} \left\{ \binom{1}{1}, \binom{1}{-1}, \binom{1}{i}, \binom{1}{-i} \right\}$$

and $\mathbf{g}_k \in \Gamma$. Since this codebook only offers a very limited choice of precoding vectors, there will remain a significant amount of MU interference at the UEs, especially in small cells with few users. Therefore, it is crucial to implement an IA receiver that exploits the knowledge about the MU interference, as opposed to an IU receiver that treats the interference as noise.

MU-MIMO in LTE Release 9 and Beyond

The LTE Releases 9 and beyond allow for MU-MIMO transmission with UE-specific reference symbols (RS) defined as TM8 (Release 9) and TM9 (Release 10). Transmission modes 8 and 9 enable the scheduling of up to four users with a single data stream or up to two users with two data streams each. The UE-specific RS are precoded the same way as the data, thus leaving the actual precoding open to implementation and entirely transparent to the UEs. Hence, the users are completely oblivious to whether the eNB applied a linear precoding technique like zero-forcing (ZF) or regularized ZF[8][9] or even a nonlinear technique such as Tomlinson-Harashima precoding. However, note that such non-codebook-based approaches require accurate downlink channel estimate at the eNB, which can only be obtained via quantized codebook-based feedback in FDD systems. Furthermore, with UE-specific RS the UE does not know if there are any co-scheduled users or if it is operating in SU-MIMO mode. If the precoding is working well, there will not be any significant MU interference and thus an IA receiver will not improve the performance compared to an IU receiver. The UE can monitor the power of the interfering streams by estimating the effective channel $\bar{\mathbf{h}}_j$ since the UE-specific RS among the potentially co-scheduled users are quasi-orthogonal. Subsequently, if the interference power $\|\bar{\mathbf{h}}_j\|^2$ exceeds some given threshold, the UE will cancel this interference with an IA receiver.

Recently 3GPP created a new study item for LTE Release 12 on Network-Assisted Interference Cancellation and Suppression (NAICS)[10] to study the potential advantages of providing additional information to the UE in order to support its interference cancellation abilities. In the context of MU-MIMO, such information could include the interfering modulation order and the number of interferers (co-scheduled users). If the UE receiver is capable of decoding and subtracting the interfering data stream, then information about the interfering Modulation and Coding Scheme (MCS) and resource allocation is required. This could be achieved by providing the UE with the Radio Network Temporary Identifier (RNTI) of the interfering users to decode the interfering DCIs and subsequently the data for successive interference cancellation.

"…It is crucial to implement an IA receiver that exploits the knowledge about the MU interference, as opposed to an IU receiver that treats the interference as noise."

In our context of TM5 and the IA receiver, the only additional information that is required, is the interfering modulation order (that is, QPSK, 16QAM, or 64QAM). The measurements presented in this article investigate how valuable this interfering modulation order is under different propagation environments.

Interference-Aware Receiver

The IA receiver design has been proposed by Ghaffar and Knopp[4] and exploits the potentially available information about the MU interference, that is, the interfering effective channels $\overline{\mathbf{h}}_j$ ($j \neq k$) and the interfering symbol alphabet A_j. In the following, we briefly review the principle of the IA receiver.

As discussed in the previous section, each user has access to the effective channels $\overline{\mathbf{h}}_j$ either through cell-specific RS and the a-priori known codebook as in LTE Release 8, or through UE-specific RS as in LTE Release 9 and beyond. Concerning the interfering symbol alphabet A_j, this information is not readily available to the UEs. The symbol alphabets A_j could be estimated from the statistics of the received signal as shown by Bae et al.[5], but this approach is computationally complex. Ghaffar and Knopp[11] always chose $A_j = Q_{16}$, independent of A_k, which is reasonable if $A_j = A_k$. However, if $A_j \neq A_k$, we observe through simulations in the subsequent section, that assuming identical alphabets, that is, $A_j = A_k$ performs very well even if the true interfering constellation is different.

To compute the log-likelihood ratios (LLRs) Λ, required as an input to the channel decoder, we apply the classical ML criterion with subsequent Max-log approximation. Without loss of generality, we focus on UE k and hence drop the index k. The minimum distance λ reads

$$\lambda = \max_{s_i \in A_i} \left\{ -\left\| \mathbf{y} - \sum_{i=1}^{K} \overline{\mathbf{h}}_i s_i \right\|^2 \right\}.$$

For $n_t = K = 2$, omitting the common term $\|\mathbf{y}\|^2$ and separating into real and imaginary parts we obtain

$$\lambda = \max_{\substack{s_1 \in A_1 \\ s_2 \in A_2}} \left\{ -\|\overline{\mathbf{h}}_1\|^2|s_1|^2 - \|\overline{\mathbf{h}}_2\|^2|s_2|^2 + 2[\overline{y}_1^R s_1^R + \overline{y}_1^I s_1^I] + 2|\eta_1\|s_2^R| + 2|\eta_2\|s_2^I| \right\} \quad (1)$$

with

$$\eta_1 = \rho_{12}^R s_1^R + \rho_{12}^I s_1^I - \overline{y}_2^R$$
$$\eta_2 = \rho_{12}^R s_1^I - \rho_{12}^I s_1^R - \overline{y}_2^I$$

where we defined the matched filter outputs $\overline{y}_1 \triangleq \overline{\mathbf{h}}_1^H \mathbf{y}$, $\overline{y}_2 \triangleq \overline{\mathbf{h}}_2^H \mathbf{y}$, and the correlation coefficient $\rho_{12} \triangleq \overline{\mathbf{h}}_1^H \overline{\mathbf{h}}_2$. Note that in Equation 1 we do not require the sign of the interfering symbol s_2 since Equation 1 is maximized if s_2^R and s_2^I have the opposite signs of η_1 and η_2, respectively. Moreover, the search space for the ML detection can be reduced by one complex dimension since both η_1 and η_2 are *independent* of s_2 and hence by equating the derivative of the expression in braces in Equation 1 to zero the optimal values of $|s_2^R|$ and $|s_2^I|$ are directly given as

$$|s_2^R|^* = \frac{\|\overline{\mathbf{h}}_2\|^2}{|\eta_1|} \; and \; |s_2^I|^* = \frac{\|\overline{\mathbf{h}}_2\|^2}{|\eta_2|}.$$

For detailed expressions of the LLRs under various symbol alphabets the reader is referred to Ghaffar and Knopp.[4]

The above IA receiver is able to cancel a *single* interferer. An extension to multi-interference cancellation is not straightforward since the optimal interference amplitude can only be directly computed for one interfering symbol. To cancel more than one interferer requires a full ML detection, which quickly increases the complexity of the receiver. But as previously mentioned, the UE can monitor the strength of the interfering users $\|\bar{\mathbf{h}}_j\|^2$ and decide to cancel the strongest interferer if beneficial.

Precoder Selection

User k selects the optimal precoding vector $\mathbf{g}_k^*$ that maximizes his desired *effective* channel magnitude $\|\mathbf{H}_k\mathbf{g}_k\|$, that is,

$$\mathbf{g}_k^* = \arg \max_{\mathbf{g} \in \Gamma}\{\|\mathbf{H}_k\mathbf{g}\|\}$$

and sends the corresponding precoding matrix indicator (PMI) to the eNB. In the test configuration presented in this article, we always assume that two users with orthogonal precoding vectors are scheduled for transmission. Moreover, the above maximization is carried out over the average channel per sub-band as opposed to wideband PMI described by Bai et al.[6]

Simulation Results

Before carrying out real-time measurements, we do link-level simulations to identify the performance loss incurred by a false assumption on the interfering symbol alphabet A_j. Given various modulation and coding schemes (MCS), we measure the Block-Error Rate (BLER) for the SCM-C channel model [12] and average over 10,000 independent channel realizations. The system parameters are given in Table 1.

|	
Carrier Frequency	1907.6 MHz
System Bandwith	5 MHz
Number of Transmit Antennas at eNB	2
TDD Configuration	3
DL Transmit Subframe	7
UL Transmit Subframe	3
RB Allocation	8191 (all 25 RBs)
Number of PDCCH symbols	1

**Table 1:** System Configuration Parameters
(Source: EURECOM, 2013)

Figure 1, Figure 2, and Figure 3 show the simulation results for QPSK, 16QAM, and 64QAM interference, respectively. From these figures it can be observed that if the desired user has a QPSK alphabet, then the assumption on

"An extension to multi-interference cancellation is not straightforward…"

the interfering constellation has little impact on the IA receiver performance. Even the IU receiver performs almost as well as the IA receiver. If the desired constellation is 16QAM or 64QAM, we observe that the performance loss is more significant, especially if the interfering modulation order is high but a low modulation order is assumed. From these simulations we conclude that
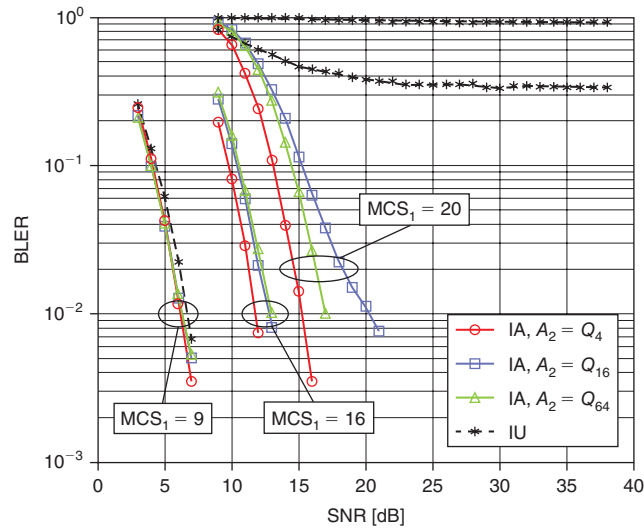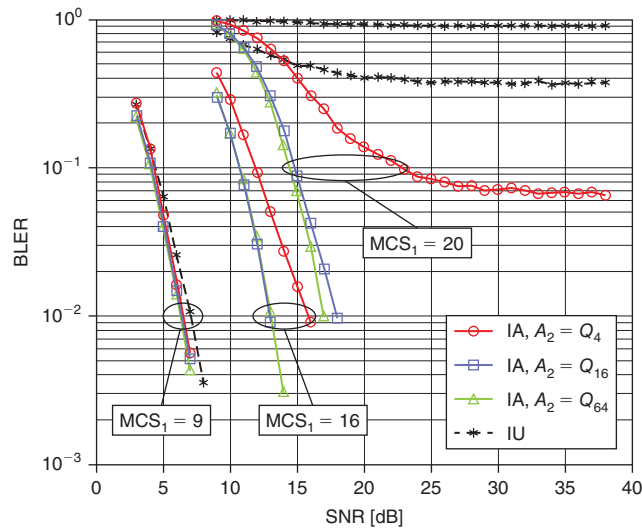

Figure 1: QPSK interference, BLER vs. SNR, $MCS_1 = \{9, 16, 20\}$, $MCS_2 = 9$, $n_r = 2$, SCM-C, no HARQ, 10,000 channel realization
(Source: EURECOM, 2013)
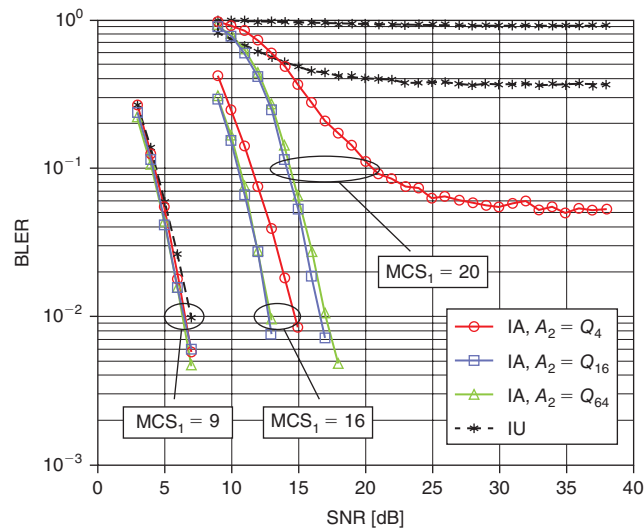
Figure 2: 16QAM interference, BLER vs. SNR, $MCS_1 = \{9, 16, 20\}$, $MCS_2 = 16$, $n_r = 2$, SCM-C, no HARQ, 10,000 channel realization
(Source: EURECOM, 2013)

Figure 3: 64QAM interference, BLER vs. SNR, $MCS_1 = \{9, 16, 20\}$, $MCS_2 = 20$, $n_r = 2$, SCM-C, no HARQ, 10,000 channel realization
(Source: EURECOM, 2013)

choosing the symbol alphabet for the interfering stream identical to the desired stream, that is, $A_j = A_k$, is robust and results only in a small performance loss. Even under a false assumption on A_j the IA receiver always outperforms the IU receiver significantly.

We are now interested in the computational complexity of the IU and IA receiver and choose to measure the processing time of each receiver on an Intel® Xeon™ CPU E5-2690 dual-core processor clocked at 3 GHz. It should be noted that the implementation makes heavy use of the Streaming SIMD Extension (SSE) 4 instruction set. The results are presented in Figure 4, where we assume that $A_1 = A_2$ and also plot the processing time of the Turbo decoder for comparison. From Figure 4, we observe that the processing time of the IU receiver increases only slightly with the modulation order, whereas the IA receiver complexity increases significantly. For 64QAM the processing time of the IA receiver is almost 5 times that of the Turbo decoder and 12 times the amount of the IU receiver. Although the IA receiver greatly increases the computational complexity at high modulation orders, it is precisely in that region where the subsequent measurements show a tremendous performance gain over the IU receiver. Note that the real-time implementation of the LLR computation uses multiple threads to meet the real-time requirements.

Real-Time Measurements

In this section we describe the real-time measurement setup and assumptions, the equipment, and the different measurement scenarios. The throughput is measured for both IU and IA receivers in TM5.

"Choosing the symbol alphabet for the interfering stream identical to the desired stream is robust and results only in a small performance loss"

"…The implementation makes heavy use of the Streaming SIMD Extension (SSE) 4 instruction set"
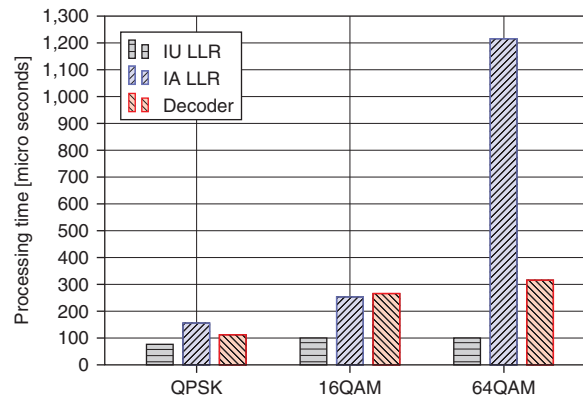
Figure 4: Processing time per subframe of the IA and IU receiver with $n_r = 2$
(Source: EURECOM, 2013)

Setup

For the test setup, we configured Time-Division Duplex (TDD) mode on LTE band 33 (1900–1920 MHz). The eNB and UE have two antennas, whereas the UE uses one antenna for transmission and one or two antennas for reception. The important system configuration parameters are summarized in Table 1.

In subframe (SF) 3, the UEs transmit their measured PMIs on the PUSCH, which is subsequently used in SF 7 by the eNB to precode the signals of both users. In our test setup, only SF 7 carries downlink data.

Note that in TM5, the data for the interfering UE (user 2) always occupies exactly the same time-frequency resources as the data for user 1, because the downlink (DL) power offset parameter, signaled in the DCI and indicating the presence of another user, is valid for the entire subframe. In TM8 and TM9, the interference could only be present partially within a codeword. The IA receiver should only be applied to those resources with interference; otherwise, in absence of interference, the IA receiver will perform worse than the IU receiver. As previously mentioned, the presence of an interfering user could be determined by monitoring the interference power and applying a suitable threshold to decide if interference cancellation is used.

In the measurements we use two IA receivers. One IA receiver assumes that the interference modulation order is the same as the desired modulation order. This receiver is simply termed "IA". The other receiver is assumed to obtain the correct interfering modulation order through network-aided (NA) signaling and is referred to as "NA-IA" receiver.

Assumptions

In the measurements, we consider the scenario where only two users are available for TM5. The eNB always uses the PMI reported by user 1 (the

"The IA receiver should only be applied to those resources with interference…"

desired user) and assigns orthogonal PMIs to user 2 regardless of the PMI report of user 2. This scheduling scheme is optimal for user 1 but suboptimal for user 2 and from a cell capacity point of view. However, since we focus on the throughput of user 1, this scheduling scheme is adequate. Note that we have only two transmit antennas at the eNB and hence use a *lower* resolution codebook than Bai et al.[6] Thus, the interference experienced by user 1 is relatively high. This assumption is realistic in small cells where the number of users is likely to be small and orthogonal PMIs might not be available, which will result in higher MU interference.

Concerning the PMI feedback, we make several assumptions. First, we ensure that the uplink (UL) is always error-free by transmitting with sufficient power. This is necessary to avoid errors in the PMI that would impair our receiver performance measurements. Secondly, we implement sub-band PMI measurements similarly to TM6, which is not foreseen in LTE Release 8 but later in Release 9 and beyond. However, this has no impact on the relative performance of the IA and IU receiver.

Since the PMI is measured in SF 2 and applied in SF 7, the channel is supposed to be approximately constant during 5 SFs or equivalently 5 ms, which was the case during the measurements.

The LTE modem ran without protocol stack (no Hybrid ARQ) and UL and DL resources were statically configured. Note that, although we disabled the higher layers for this measurements, a similar MU-MIMO setup has been successfully demonstrated with complete protocol stack during the SAMURAI project.[13][14]

During the measurements, the receiver type is changed per frame, and MCS_1 is random and uniformly distributed between 0 and 27. To make MCS_2 available to the NA-IA receiver without explicit signaling, it is coupled to the system frame number (SFN) as $MCS_2 = SFN\ mod\ 28$. Although MCS_2 is not truly random, no significant change in performance compared to a random MCS_2 has been observed. Moreover, each of the subsequent results was obtained by measuring over a time period of about 2 minutes.

Equipment

The measurements are carried out with the EURECOM experimental OpenAirInterface (OAI) platform. The OAI implements a software-defined radio of the 3GPP LTE Release 8.6 standard, which runs on common x86 Linux machines. To ensure real-time operation, we utilize the real-time application interface (RTAI). Furthermore, the real-time signals are transmitted via the PCI Express interface to the EURECOM Express MIMO 2 board (see Figure 5), where the base-band signal is modulated and transmitted via an additional RF front-end as depicted in Figure 6. The Express MIMO 2 board is able to receive and transmit on four channels independently and for a wide range of frequencies.

"…a similar MU-MIMO setup has been successfully demonstrated with complete protocol stack during the SAMURAI project"

"The OAI implements a software-defined radio of the 3GPP LTE Release 8.6 standard, which runs on common x86 Linux machines"
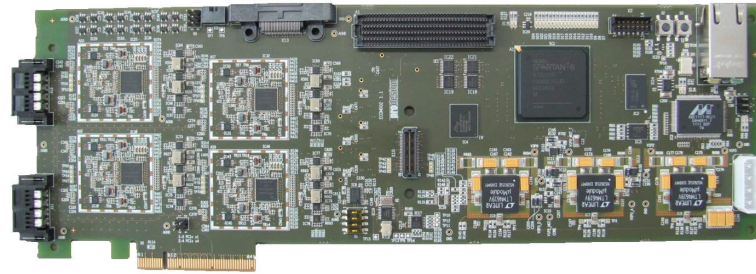
Figure 5: Express MIMO 2 board
(Source: EURECOM, 2013)

Figure 6: User equipment with RF board
(Source: EURECOM, 2013)

Scenarios

We consider three different scenarios:

1. Indoor scenario (UE is inside building, eNB is outside) to measure throughput for different number of receive antennas

2. Outdoor scenario with a strong line-of-sight (LOS) channel

3. Outdoor scenario with non-LOS (NLOS) channel conditions

In all scenarios the UE is moved at low speeds to avoid a strong Doppler effect but to allow for an averaging of the performance over sufficiently different channel realizations.

Measurement Results

The throughput measurements for all three scenarios are presented in the following sections.

### Indoor Scenario with Variable Number of Receive Antennas

The measurement setup consists of an eNB situated outside on top of the EURECOM building and the UE placed inside the building.

Figure 7 and Figure 8 show the average throughput of IU, IA, and NA-IA receivers with one or two receive antennas, respectively, for different values of MCS_1. From these figures we observe that, for QPSK (that is, MCS 0,1,…,9),
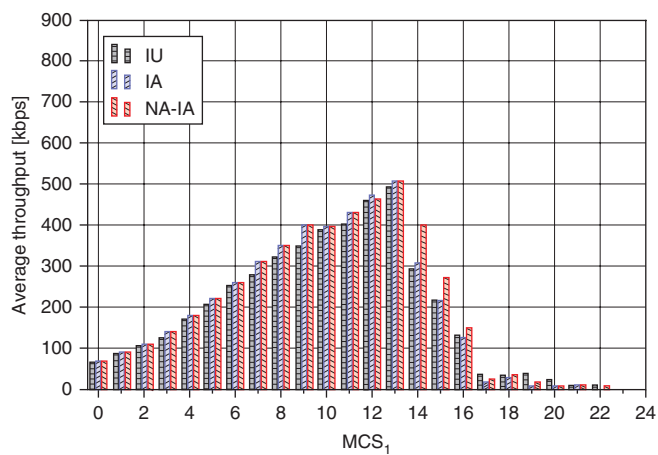
Figure 7: MCS_1 vs. average throughput with $n_r = 1$, indoor scenario
(Source: EURECOM, 2013)
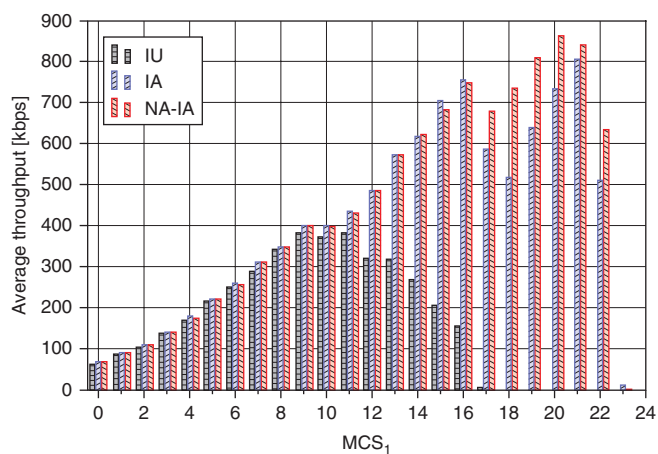
Figure 8: MCS_1 vs. average throughput with $n_r = 2$, indoor scenario
(Source: EURECOM, 2013)

"With two receive antennas the performance of the IA and NA-IA receivers improve drastically…"

all receivers achieve about the same throughput irrespective of the number of receive antennas.

From Figure 7, we observe that the IA receiver does not offer a significant throughput increase if only a single receive antenna is available. However, the NA-IA receiver can achieve moderately higher throughput for higher MCS.

With two receive antennas the performance of the IA and NA-IA receivers improve drastically (see Figure 8), whereas the IU receiver shows a small performance loss, which may be explained by the varying channel conditions. The NA-IA receiver outperforms the IA receiver for $MCS_1 > 16$, that is, for 64QAM.

We conclude that an IA receiver can significantly improve the performance of the UE in TM5, especially if an additional receive antenna is present to allow for effective interference mitigation. Furthermore, the NA-IA receiver can improve the performance if 64QAM is used.

Outdoor Scenario with Strong Line-of-Sight Component

Figure 9 shows the measurement environment with the UE in the foreground and the eNB on the roof in the background. During the measurement we move the UE slowly in one direction and back multiple times.

Figure 9: Outdoor scenario with strong LOS channel
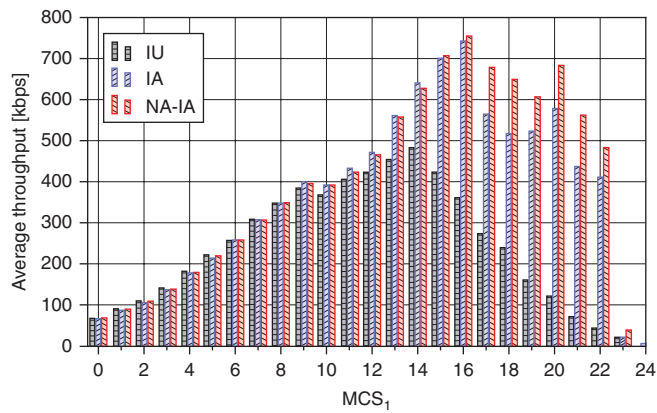(Source: EURECOM, 2013)

Figure 10 depicts the measurement results for all three receivers. It can be observed that both IA and NA-IA receivers achieve maximum throughput for $MCS_1 = 16$ and the IU receiver at $MCS_1 = 14$. Although the maximum throughput of IA and NA-IA receivers are almost identical, the NA-IA receiver achieves a significantly higher throughput for $MCS_1 > 16$, that is, for 64QAM.

"…The NA-IA receiver achieves a significantly higher throughput for 64QAM"

Outdoor Scenario without Line-of-Sight Component

Figure 11 shows the NLOS environment, where the UE was slowly moved straight until the bridge.

Figure 10: MCS_1 vs. average throughput with $n_r = 2$, outdoor scenario with strong LOS channel
(Source: EURECOM, 2013)

Figure 11: NLOS environment with eNB on the roof of right building
(Source: EURECOM, 2013)

The throughput results for a NLOS channel are presented in Figure 12. It can be seen that the difference in maximum throughput between IA and NA-IA receivers is negligible and almost identical compared to the results in the LOS environment. Moreover, as in the LOS channel, the NA-IA receiver significantly outperforms the IA receiver for 64QAM modulation. These results suggest that the *relative* performance of IA and NA-IA receivers is robust to the propagation environment, that is, their throughput difference is similar in LOS and NLOS channels.
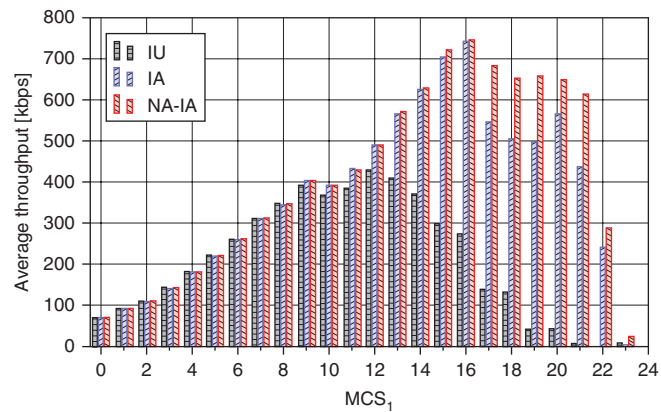
Figure 12: MCS_1 vs. average throughput with $n_r = 2$, outdoor scenario with non-LOS channel (Source: EURECOM, 2013)

Regarding the IU receiver, we observe significant performance degradation in NLOS compared to LOS channels, especially for $MCS_1 > 12$. For instance, the maximum throughput in LOS of 481 kbps decreased to 428 kbps in the NLOS channel. Even more drastic is the loss at higher order modulations, for example, for $MCS_1 = 17$ the throughput decreased from 273 kbps to 137 kbps. We conclude that the IU receiver benefits significantly from LOS environments, especially at higher order modulations. This is in line with the findings of Bai et al.[6], who showed that channel correlation is beneficial for MU-MIMO. The LOS component of the channel increases the channel correlation and hence renders the precoding more effective, resulting in lower MU interference.

"The IU receiver benefits significantly from LOS environments, especially at higher order modulations"

Conclusion

This article evaluated the potential performance improvements of IA receiver designs over an IU receiver in TM5 through real-time field measurements in LOS and NLOS propagation environments.

In the case of a single receive antenna, the measurements indicate that the IA receiver offers almost no advantage compared to the IU receiver.

However, for both single- and dual-receiver antennas, the measurements revealed that the NA-IA receiver significantly outperforms the IA receiver

for higher order modulations, such as 64QAM. This result suggests that the signaling of the interfering modulation order can greatly improve performance in the case where 64QAM is applied. For lower order modulations the simplified IA receiver without knowledge of the interfering modulation order performs equally well as the NA-IA receiver.

Moreover, the measurements indicate that the IU receiver benefits significantly from LOS channels compared to the IA receivers, especially at higher order modulations. In the case of QPSK, even the IU receiver achieves the same throughput as the IA receivers.

We conclude that a UE with IA receiver can greatly increase both cell and user throughput, especially with additional network assistance.

"…A UE with IA receiver can greatly increase both cell and user throughput, especially with additional network assistance"

References

[1]   3rd Generation Partnership Project, "Physical Channels and Modulation," 3GPP TS 36.211 V8.6.0, 2009.

[2]   Sesia, S., I. Toufik, and M. Baker, *LTE, The UMTS Long Term Evolution: From Theory to Practice,* 2 ed., Wiley & Sons, 2011.

[3]   Duplicy, J. B. Badic, R. Balraj, R. Ghaffar, P. Horvath, F. Kaltenberger, R. Knopp, I. Z. Kovács, H. T. Nguyen, D. Tandur, G. Vivier, "MU-MIMO in LTE systems," *EURASIP Journal on Wireless Communications and Networking*, 2011.

[4]   Ghaffar, R. and R. Knopp, "Interference-Aware Receiver Structure for Multi-user MIMO and LTE," *EURASIP Journal on Wireless Communications and Networking*, no. 1, pp. 1-17, 2011.

[5]   Bae, J. H., S. Kim, J. Lee, and I. Kang, "Advanced Downlink MU-MIMO Receiver for 3GPP LTE-A," in *IEEE International Conference on Communications (ICC)*, 2012.

[6]   Bai, Z., S. Iwelski, G. Bruck, P. Jung, B. Badic, T. Scholand, and R. Balraj, "Receiver Performance-Complexity Tradeoff in LTE MU-MIMO Transmission," in *Ultra Modern Telecommunications and Control Systems and Workshops (ICUMT)*, 2011.

[7]   EURECOM, "OpenAirInterface Hardware/Software Development Platform," Sep 2013. [Online]. Available: http://www.openairinterface.org.

[8]   Peel, C. B., B. M. Hochwald, and A. L. Swindlehurst, "A Vector-perturbation Technique for Near-Capacity Multiantenna Multiuser Communication - Part I: Channel Inversion and Regularization," *IEEE Transactions on Communications*, vol. 53, no. 1, pp. 195-202, 2005.

[9]   Wagner, S., R. Couillet, M. Debbah, and D. T. Slock, "Large System Analysis of Linear Precoding in Correlated MISO Broadcast Channels under Limited Feedback," *IEEE Transactions on Information Theory*, vol. 58, no. 7, pp. 4509-4537, 2012.

[10]   3rd Generation Partnership Project, "Network-Assisted Interference Cancellation and Suppression for LTE (Release 12)," 3GPP TR 36.866, 2013.

[11]   Ghaffar, R. and R. Knopp, "Interference Sensitivity for Multiuser MIMO in LTE," in *IEEE 12th International Workshop on Signal Processing Advances in Wireless Communications (SPAWC)*, 2011.

[12]   3rd Generation Partnership Project, "Spatial Channel Model for Multiple Input Multiple Output (MIMO) Simulations," TR 25.996, 2009.

[13]   Badic, B., A. F. Cattoni, M. Dieudonne, J. Duplicy, P. Fazekas, F. Kaltenberger, I. Z. Kovács, and G. Vivier, "Advances in Carrier Aggregation and Multi-User MIMO for LTE-Advanced: Outcomes from SAMURAI project," http://www.ict-samurai.eu/content/publications, 2012.

[14]   Cattoni, A. F., H. T. Nguyen, J. Duplicy, D. Tandur, B. Badic, R. Balraj, F. Kaltenberger, I. Latif, A. Bhamri, and G. Vivier, "Multi-user MIMO and Carrier Aggregation in 4G systems: The SAMURAI Approach," in *IEEE Wireless Communications and Networking Conference Workshops (WCNCW)*, 2012.

Acknowledgements

Author Biographies

Sebastian Wagner is an LTE firmware engineer at Intel Mobile Communications since 2013. He received his MS in Electrical Engineering from the Technische Universität Dresden in 2008 and the PhD from Télécom ParisTech (EURECOM) in 2011. He joined EURECOM as a post-doctoral fellow in 2012 where he was involved in the LTE Modem development for the OpenAirInterface platform. His research interests include signal processing, MIMO communication systems, receiver design and the application of random matrix theory to wireless communications. He can be contacted at sebastian.wagner@intel.com.

Florian Kaltenberger is an Assistant Professor in Mobile Communications at EURECOM and part of the team managing the real-time open-source test platform OpenAirInterface.org for experimentation in LTE systems. He

received his MS and his PhD both in Technical Mathematics from the Vienna University of Technology in 2002 and 2007, respectively. His research interests include signal processing for wireless communications, MIMO communication systems, receiver design and implementation, MIMO channel modeling and simulation, and hardware implementation issues. He can be contacted at florian.kaltenberger@eurecom.fr.